Colloidal dynamics in polymer solutions: Optical two-point microrheology measurements

Laura Starrs and Paul Bartlett*

School of Chemistry, University of Bristol, Bristol, UK BS8 1TS.
E-mail: P.Bartlett@bristol.ac.uk

We present an extension of the two-point optical microrheology technique introduced by Crocker *et al.* [J. C. Crocker, M. T. Valentine, E. R. Weeks, T. Gisler, P. D. Kaplan, A. G. Yodh and D. A.Weitz, *Phys. Rev. Lett.*, 2000, **85**, 888 (ref. 7)] to high frequencies. The correlated fluctuations of two probe spheres held by a pair of optical tweezers within a viscoelastic medium are determined using optical interferometry. A theoretical model is developed to yield the frequency-dependent one- and two-particle response functions from the correlated motion. We demonstrate the validity of this method by determining the one- and two-particle correlations in a semi-dilute solution of polystyrene in decalin. We find that the ratio of the one- and two-particle response functions is anomalous which we interpret as evidence for a slip boundary condition caused by depletion of polymer from the surface of the particle.

I.   Introduction

The dynamics of colloidal particles dispersed in viscoelastic polymer solutions are important in both fundamental and applied science. Suspensions of particles in polymers are encountered in a vast range of chemical products including coatings, controlled-release drug formulations, personal care products, and filled polymer composites as well as being significant in many biological processes, such as intracellular transport inside the viscoelastic cytoplasm of a cell.[1] From a fundamental viewpoint, the characteristic lengths of polymers and colloids which differ by several orders of magnitude, suggest that these mixtures should be ideal candidates for coarse-grained descriptions. However while such approaches have been applied to equilibrium properties with considerable success there have been no comparable attempts, so far, to explain and quantify the rich dynamical and rheological properties of these complex mixtures. Understanding the dynamics of these complex systems remains an important goal of soft matter science. In recent years considerable experimental progress in the characterization of these systems has been made though the development of optical microrheology techniques. The underlying idea, pioneered by Mason and Weitz,[2] is that the Brownian fluctuations of a colloidal probe particle reflect the viscoelasticity of the medium in which the probe is embedded. By analysing the thermal motion it is possible to obtain quantitative information about the rheological properties of the polymer matrix over an extended range of frequencies not accessible to conventional rheometers. Optical microrheology experiments typically monitor the thermal fluctuations of a *single* probe particle using a combination of video microscopy, optical interferometry,[3,4] or diffusing wave spectroscopy.[2] While microrheological techniques enjoy significant potential advantages over traditional rheological

methods complications in interpretation have limited their application.[5] The problem is that the presence of a particle can perturb the surrounding medium (by, for instance, depleting polymer segments from near the particle surface) so that the dynamics of a single particle fails to reflect the macroscopic viscoelasticity of the medium.[6,7] In effect, a particle diffuses in a "pocket" of material whose local rheological properties are not those of the bulk. To circumvent this limitation, Crocker *et al.*[7] conjectured that the correlated fluctuations of *two* separated probe particles should measure the bulk rheological properties of inhomogeneous materials more accurately than traditional one-particle experiments. Using video microscopy they tracked the thermal diffusion of pairs of probe particles embedded in a viscoelastic solution of guar and confirmed that the extracted viscoelastic moduli were in close agreement with conventional measurements. Significantly, the single particle results differed substantially, both in magnitude and scaling, from the two-particle results. Recently these observations have been confirmed theoretically by Levine and Lubensky.[8] Using an analogy to classical electrostatics they have shown that while one-point techniques measure essentially a local rheology, two-point correlations determine the bulk rheology. Interestingly, these observations suggest that combined one- and two-point measurements could be a powerful tool to probe the nature of the specific interactions between particle and medium.

In this paper, we present an extension of the two-point correlation technique to high frequencies using optical interferometry to track particles with high spatial and temporal resolution. Our approach allows access to a much faster range of timescales than previous measurements,[7] as we show later. In consequence we are able to measure the rheological properties in a frequency range from typically $\sim 10^1$ to 10^4 rad s^{-1}. Accurate measurements of multi-point correlations are substantially more demanding than one-point measurements. To achieve adequate signal-to-noise levels we have been forced to use a more intense laser beam than usually employed in particle tracking experiments.[1,3,4] We consider explicitly the effects of optical-gradient forces and assume that each particle is held within a fixed harmonic potential. The two-particle correlations measured therefore differ from those discussed by Crocker *et al.*[7] where diffusion occurs in the absence of a potential. We develop a generalised Langevin theory to account for the correlated time-dependent fluctuations in terms of the viscoelasticity of the medium. Our paper is organised as follows: In Section II, we present an analysis of our two-particle microrheology experiments, and discuss how two-particle correlations are related to the viscoelasticity of the medium (Section IIB). Next, in Section III we describe our experimental setup and numerical procedures. Finally in Section IV we present measurements of one- and two-point fluctuations of two widely-spaced spheres immersed in a semi-dilute polymer solution which demonstrate the validity of our approach before we conclude in Section V.

II.   Theory

The fundamental concept underlying optical microrheology experiments is that the Brownian motion of a rigid spherical tracer particle is determined by the viscoelasticity of the surrounding medium. Typically the mean-squared displacement (MSD) $\langle \Delta x^2(t) \rangle = \langle [x(t) - x(0)]^2 \rangle$ of the particle trajectory is measured (here $x(t)$ denotes the tracer particle position after a time t and the brackets denote a time or ensemble average). The MSD is related to the rheological properties of the medium though linear response theory. In general, the time-dependent frictional force $F(t)$ on a sphere moving with a velocity $u(t)$ through a viscoelastic medium may be written as[9]

$$ F(t) = \int_{-\infty}^{t} \xi(t - t')u(t')\mathrm{d}t', \qquad (1) $$

where $\xi(t)$ is the instantaneous friction coefficient. The convolution on the right hand side of eqn. (1) reflects the viscoelastic nature of the suspending fluid. Energy is stored as the Brownian particle diffuses, generating a "memory" of the particle's past motion. In consequence, the frictional force experienced at a time t depends on the particle velocity at all earlier times t'. This non-local time-dependence changes profoundly the Brownian trajectory so that from a measurement of the MSD the time-dependent friction coefficient $\xi(t)$ can be determined. The utility of microrheological measurements depend on extracting information about the rheological properties of the medium from the time dependence of $\xi(t)$. Below we show how the time- or more conveniently the

frequency-dependent *pair* friction coefficients may be determined from the correlated fluctuations of two widely-separated tracer particles held by a pair of optical traps. We then review the connection between the two-particle friction coefficients and the rheology of the medium.

A.   Correlated Brownian motion in a viscoelastic fluid

The optical gradient forces on a high refractive-index particle within a tightly-focused laser beam are well approximated by a harmonic interaction. Consequently, we model our experiments by analysing the dynamics of a pair of rigid Brownian particles of radius a, each held in a harmonic potential well, and separated by a distance r within a linear viscoelastic medium. Fluctuations in the positions of the two particles are correlated as a result of the hydrodynamic interactions which are transmitted through the viscoelastic matrix. The standard Langevin description (see for instance refs. 10 and 11) for the Brownian motion of a pair of neutrally-buoyant particles of mass m is readily modified to include the effects of the viscoelasticity of the medium,

$$m\frac{\mathrm{d}u_1(t)}{\mathrm{d}t} = -\int_{-\infty}^{t} \xi_{11}(t-t')u_1(t')\mathrm{d}t'$$
$$-\int_{-\infty}^{t} \xi_{12}(t-t')u_2(t')\mathrm{d}t' - kx_1(t) + f_1^R(t)$$
$$m\frac{\mathrm{d}u_2(t)}{\mathrm{d}t} = -\int_{-\infty}^{t} \xi_{22}(t-t')u_2(t')\mathrm{d}t'$$
$$-\int_{-\infty}^{t} \xi_{21}(t-t')u_1(t')\mathrm{d}t' - kx_2(t) + f_2^R(t). \tag{2}$$

Here the subscripted indices label the two Brownian spheres, k is the harmonic force constant of the optical traps (assumed identical), and $f_i^R(t)$ denotes the random Brownian forces acting on particle i ($i = 1,2$). The time-dependent frictional coefficients $\xi_{ij}(t)$ in eqn. (2) result from the generalisation of the viscoelastic "memory" (eqn. (1)) to the case of two interacting particles. The self term $\xi_{11}(t)$ details the force acting on one sphere when the same sphere is moving (and the second sphere is stationary) while the cross friction coefficient $\xi_{12}(t)$ describes the force generated on one sphere by the motion *alone* of the other sphere. Since the random thermal and frictional forces both have the same microscopic origin they must satisfy in equilibrium at a temperature T, the fluctuation–dissipation theorem $\langle f_i^R(t) f_j^R(t')\rangle = k_B T \xi_{ij}(t-t')$.[12]

The coupled generalized Langevin eqn. (2) is simplified by introducing collective and relative normal coordinates and using standard techniques to solve the resulting decoupled equations of motion. Here we focus on the solution for the two-particle mean-squared displacement, namely

$$d_{ij}(t) = \frac{\langle \Delta x_i(t) \Delta x_j(t)\rangle}{\sqrt{\langle \Delta x_i^2\rangle \langle \Delta x_j^2\rangle}}, \tag{3}$$

where the displacements are normalised by the equipartition result, $\langle \Delta x_i^2\rangle = 2k_B T/k$. The mutual two-particle mean-squared displacement $d_{ij}(t)$ for $i \neq j$ details the correlation between the thermal fluctuations of the two separated particles. The self term $d_{ii}(t)$, is the MSD of particle i in the presence of a second particle. The exact solution for the two-particle displacement function is from eqn. (2),

$$\tilde{d}_{ij}(s) = \frac{k}{2}\left[\frac{1}{s^3 m + s^2\tilde{\xi}_+ + sk} + \frac{2\delta_{ij}-1}{s^3 m + s^2\tilde{\xi}_- + sk}\right], \tag{4}$$

where the tilde denotes a Laplace transform, $\tilde{f}(s) = \int_0^\infty f(t)\mathrm{e}^{-st}\mathrm{d}t$, s is the Laplace variable and $\tilde{\xi}_\pm = \tilde{\xi}_{11} \pm \tilde{\xi}_{12}$. The complete solution eqn. (4) is still too complicated to use to analyse experimental data. In order to derive a simpler result we make two simplifying assumptions.

We start by considering the importance of particle inertia. The mass m of the particle determines the decay time $\tau_B \sim m/6\pi\eta_\infty a$ of the particle velocity autocorrelation function. Here η_∞ is the high frequency viscosity of the medium. For frequencies small compared to $\omega_B = 1/\tau_B$ the momentum

of the Brownian particle will have relaxed to zero and we may neglect particle inertia. In our experiments, ω_B is of order 10 MHz so neglecting particle inertia is an excellent approximation at frequencies of experimental interest ($\omega \leqslant 20$ kHz).

Secondly, we consider only the situation where the two probe spheres are separated by a distance r which is large in comparison to the sphere radius a. In this limit, Batchelor[13] has argued from general symmetry considerations that the hydrodynamic functions depend on the dimensionless sphere separation $\rho = r/a$ as,

$$\xi_{11} = a_0 + \frac{a_2}{\rho^2} + \frac{a_4}{\rho^4} + \mathcal{O}(\rho^{-6})$$

$$\xi_{12} = -\frac{b_1}{\rho} - \frac{b_3}{\rho^3} - \mathcal{O}(\rho^{-5}) \tag{5}$$

where the coefficients a_i and b_i are constants for a given medium. This asymptotic solution reveals that provided the two spheres are far enough apart, the self friction ξ_{ii} is, to leading order, independent of the separation ρ. The mutual friction coefficient ξ_{12} by contrast depends sensitively on the pair separation varying as $1/\rho$ at large r so that the ratio ξ_{12}/ξ_{11} is a small parameter which shrinks with increasing separation as $1/\rho$. Consequently the exact expression for the two-particle displacements (eqn. (4)) may be simplified by expanding $\tilde{d}_{ij}$ in powers of $\tilde{\xi}_{12}/\tilde{\xi}_{11}$. At large ρ, only the constant terms and the part which decays with distance as $1/\rho$ contribute to the displacement field. Retaining these leading terms yields the desired simplified expression for the correlated sphere displacements. Ignoring particle inertia, the one- and two-particle displacements may then be expressed as

$$\tilde{d}_{ii}(s) = \frac{k}{s(s\tilde{\xi}_{ii} + k)}$$

$$\tilde{d}_{ij}(s) = -\frac{k\tilde{\xi}_{ij}}{(s\tilde{\xi}_{ii} + k)^2}, \tag{6}$$

where $i \neq j$. Rearranging these equations gives expressions for the friction coefficients in terms of experimental quantities, namely

$$\frac{s}{k}\tilde{\xi}_{ii}(s) = \frac{1}{s\tilde{d}_{ii}(s)} - 1$$

$$\frac{s}{k}\tilde{\xi}_{ij}(s) = \frac{-\tilde{d}_{ij}(s)}{s\tilde{d}_{ii}^2(s)}. \tag{7}$$

Measurements of the single-particle fluctuations yield the self friction $\tilde{\xi}_{ii}(s)$, whereas the mutual friction coefficient is found from a knowledge of both single-particle and two-particle positional fluctuations. Our analysis is valid for any viscoelastic media, we make no assumptions about the homogeneity of the medium. We assume only that: (i) the particle pair separation r is large in comparison to the sphere radius a, and (ii) particle inertia is unimportant.

B. Relation to rheology

The relationship between the friction coefficient $\tilde{\xi}_{ij}(s)$ and the viscoelasticity of the medium is a challenging problem in fluid mechanics. Some of the complications are illustrated in Fig. 1 which shows schematically the microstructure of a colloid-polymer mixture. If the polymer is non-adsorbing then around each particle is a depletion zone of width ζ where the polymer concentration is less than in the bulk. Physically, we expect the motion of an individual sphere to depend on the *local* environment rather than the rheology of the bulk solution. So it seems reasonable to expect the depletion zone around a particle to speed up diffusion, in comparison to the case where the medium is homogeneous. While such specific interactions between probe and medium have not been considered, Levine and Lubensky[8] have analysed in detail the simpler case of a viscoelastic continuum. Over a wide range of frequencies, they predict that the single particle friction coefficient satisfies the generalised Stokes–Einstein relation,
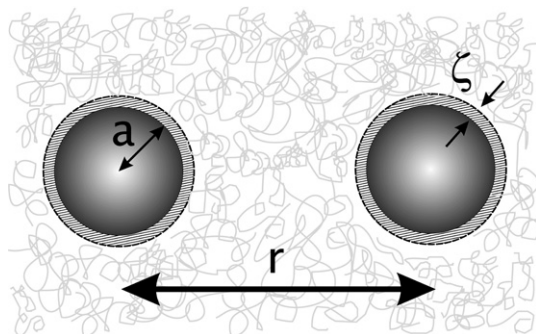
Fig. 1 Schematic illustration of two-point microrheology. Two spheres of radius a are suspended a distance r apart in a semi-dilute polymer solution. The non-adsorbing polymer is depleted from an interfacial region of width ζ surrounding each particle (shown hatched). The dynamics of an individual particle is a sensitive function of the width and properties of the interfacial zone. By contrast, the correlated *pair* fluctuations depend upon the mechanical properties of the medium, averaged on the longer scale r. In the limit when $r \gg a \gg \zeta$ the pair fluctuations measure the bulk rheology.

$$\tilde{\xi}_{ii}(s) = \frac{6\pi a \tilde{G}(s)}{s}, \tag{8}$$

where $\tilde{G}(s)$ is the Laplace shear modulus of the homogeneous medium. This result reduces to the well-known Stokes expression ($\xi = 6\pi\eta a$) for the friction of a rigid sphere in a viscous fluid[9] if the Laplace modulus is replaced by its Newtonian limit, $\tilde{G}(s) = s\eta$. Deviations from eqn. (8) are expected if the local environment around each sphere is not the same as the bulk.

While probe–particle interactions have a significant effect on single particle motion, Crocker et al.[7] have suggested that they should have a much weaker influence on the correlated fluctuations of *pairs* of particles. This conjecture has recently been confirmed theoretically.[8] Physically this is because the hydrodynamic forces operating between particles separated by a distance r reflect an average on a scale r, which is large in comparison to the width of the inhomogeneous zone ζ around each sphere. In a homogeneous viscoelastic medium, the two-particle friction coefficient has the form,

$$\tilde{\xi}_{ij}(s) = -\frac{9\pi a \tilde{G}(s)}{\rho s}. \tag{9}$$

This equation is valid provided the pair separation r is large in comparison to the sphere radius a. In the Newtonian limit, we recover the asymptotic form of the mutual friction coefficient for a viscous fluid ($\xi_{ij} = -9\pi\eta a/\rho$).[13]

III.   Materials and methods

A.   Dual-beam optical tweezers

The details of the dual-beam optical tweezer equipment used in the present experiments have been described in a preceding publication.[11] Fig. 2 shows schematically the apparatus. In brief, two spherical colloidal particles are held by optical gradient forces near the focus of a pair of ortho-gonally-polarised laser beams ($\lambda = 1064$ nm). The mean separation r between the probe particles was varied by altering the positions of the trapping lasers with an external computer-controlled mirror. The thermal fluctuations in the position of each probe particle were monitored by recording the interference between the forward scattered and transmitted infra-red beams with a pair of quadrant photodetectors. Custom-built current-to-voltage converters allowed the in-plane positions of both spheres to be recorded with a spatial resolution of $\sim$1 nm at time intervals of 50 μs.

The optical gradient force on a sphere displaced from the focus of the laser beam is harmonic. The force constant k of each trap was determined in a separate calibration experiment.[11] Colloidal
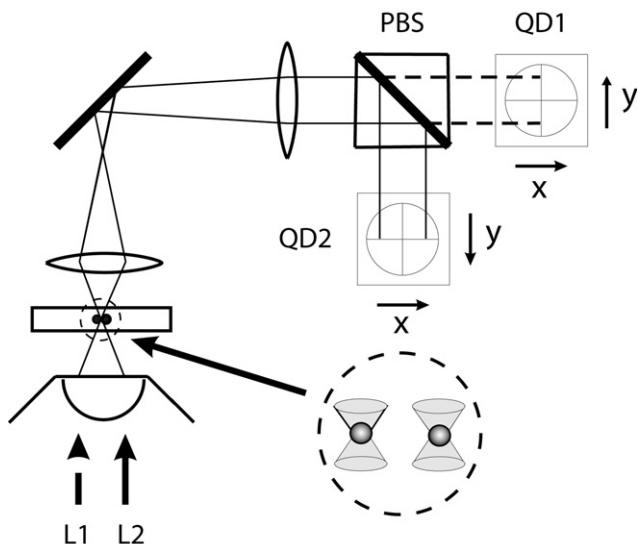
Fig. 2 Dual-beam optical tweezer setup: Optical traps are generated by focusing two orthogonally-polarized IR laser beams (L1 and L2) using a high numerical aperture microscope objective. Intensity shifts caused by interference between the direct beam and light scattered by the trapped sphere are imaged onto a pair of quadrant detectors (QD1 and QD2). A polarizing beam splitter (PBS) is used to separate the two orthogonal signals. The x and y positions are derived by combining the voltages from the four segments of the quadrant photodiodes using low-noise analog electronics. The signals are then digitized and stored on a PC.

spheres dispersed in decalin were trapped in each of the two beams in turn. The single particle mean squared displacement $\langle \Delta x^2(t) \rangle$ was measured and fitted to $\langle \Delta x^2(t) \rangle = \langle \Delta x^2 \rangle [1 - \exp(-t/\tau)]$ to yield the trap stiffness $k = 6\pi\eta a/\tau$ from known values of the particle radius a and solvent viscosity η. The intensity of the two lasers was adjusted until the stiffness of the traps differed by less than $\sim 5\%$. For a given geometry and laser intensity, the harmonic force constant k is a function only of the refractive index mismatch between particle and medium, so these calibration constants are expected to hold for the polymer data presented below. The root-mean-square fluctuation in the particle position in each trap was *ca.* 50 nm.

B. Numerical methods

The normalised one- and two-particle mean-squared displacements $d_{ij}(t)$ were calculated from the measured particle trajectories $\{x_1(t), x_2(t)\}$ using fast Fourier transform algorithms.[11] The Laplace transform of the one-particle MSD $d_{ii}(t)$ was determined from a regularised fit to a linear super-position of exponential terms,

$$d_{ii}(t) = 1 - \sum_{k=1}^{N} L_k e^{-t/\tau_k}, \tag{10}$$

where N is the number of terms, τ_k is the decay time specified on a logarithmic grid and the coefficients L_k were determined by requiring that the spectrum of relaxation times remain smooth and penalizing sums proportional to their second derivative.[14] The curvature penalty suppresses unphysical wild oscillations in the solution. The constrained regularised solution to eqn. (10) was found using the CONTIN algorithm.[15] Once L_k have been determined the Laplace transform may be calculated exactly as,

$$\tilde{d}_{ii}(s) = \frac{1}{s} - \sum_{k=1}^{N} L_k \frac{1}{s + \tau_k^{-1}}. \tag{11}$$

The Laplace transform of the two-particle MSD $d_{ij}(t)$ was evaluated by a two step numerical procedure. First, $d_{ij}(t)$ was fitted to a series of cubic polynomial splines. The contribution to the transform from each time interval was then expressed in terms of a series of incomplete gamma functions which were evaluated numerically. Tests showed that errors in the transform were of the order of 5%, except near the frequency extremes where truncation errors became more significant.

IV. Results

To test our approach we have made measurements on a viscoelastic semi-dilute solution of polystyrene (PS) with an average molecular weight of 10^7 ($M_W/M_N = 1.19$) in a mixed *cis*- and *trans*-decalin solvent (volume fraction *cis*-decalin 0.48). Linear polystyrene in decalin is a well studied system.[16] The Θ-temperature of PS in an equal volume mixture of *cis*- and *trans*-decalin is $\sim16\,^{\circ}$C so at the temperature of our measurements ($\sim23\,^{\circ}$C) decalin remains a near-Θ solvent. Using literature values[16] we estimate the polymer radius of gyration at $23\,^{\circ}$C as $R_g \sim 102$ nm, slightly larger than the value under Θ-conditions of 87 nm. The overlap concentration c^* is 3.7 mg cm^{-3}. Sterically-stabilised poly(methyl methacrylate) spheres of radius $a = 0.643$ µm were added as probe particles at a volume fraction $\phi \approx 10^{-6}$. The viscous suspensions were loaded into flat, rectangular capillary tubes 170 µm thick which were hermetically sealed with a fast-setting epoxy glue and mounted onto a microscope slide. The samples were left for at least forty minutes to allow the particles to settle to the bottom surface before the beginning of an experiment. The trajectories of two spheres were collected at ten roughly even-spaced pair separations between 3 µm and 17 µm. 2^{23} data points were collected at each separation at a sampling frequency of 20 kHz. To avoid wall effects, we analysed only spheres at least 15 µm away from the capillary walls. All measurements were performed at room temperature.

The time-dependent trajectory of a sphere diffusing in a PS solution is illustrated in Fig. 3. In contrast to cross-linked gels, the entanglements present in a semi-dilute polymer solution are only temporary so on a sufficiently long time scale the solution is expected to be purely viscous. Consequently the trajectory, when averaged over a long enough period, will depend only on the external potential and not on the viscoelasticity of the solution. The optical forces are harmonic so that at long times the particle probability distribution will be Gaussian and the mean squared displacement will plateau at the equipartition limit, $\langle \Delta x^2(t) \rangle = 2k_B T/k$. This behaviour is seen in Fig. 3(d). At short times, the particle statistics are also Gaussian although diffusion is now hindered by the temporary entanglements found in the surrounding semi-dilute polymer solution (Fig. 3(a)). The non-Gaussian dynamics at intermediate times (Fig. 3(b) and (c)) are most intriguing. The trajectory is highly anisotropic and does not resemble the isotropic diffusion seen on either shorter or longer time intervals. The particle seems to make infrequent large ''jumps'' over a distance which is comparable to the polymer radius of gyration. This behaviour suggests that the instantaneous micro-environment around each sphere in a polymer solution is heterogeneous and evolves in time.

To characterise the mechanical environment in detail we calculated the mean-squared x-displacement, $\langle \Delta x^2(t) \rangle$, from the trajectory of a single particle. The data were recorded from a *pair* of widely-separated spheres trapped within a PS solution. Fig. 4 depicts one of the two MSDs, normalised by the plateau displacement, at a number of different pair separations. Data for the second sphere were essentially identical and are not shown. As expected, there is no systematic dependence of the single particle MSD on the pair separation r, provided the two spheres remain well separated ($r \gg a$). The measured $\langle \Delta x^2(t) \rangle$ is sensitive only to the local rheological environment around each particle. Because of the high frequency elasticity of the polymer solution, $\langle \Delta x^2(t) \rangle$ increases approximately as $t^{0.8}$ at early times rather than linearly, as expected for diffusion in a purely viscous medium. At long times $\langle \Delta x^2(t) \rangle$ reaches the equipartition plateau.

Using the same trajectory data, we have also calculated the two-point correlations. We expect that for widely-spaced particles the strength of the correlated positional fluctuations will decay inversely with the particle spacing. To confirm this, we plot in Fig. 5 the mutual mean-squared displacement $d_{ij}(t)$ multiplied by the dimensionless spacing ρ. The data measured for a range of different pair spacings is seen to collapse onto a common curve over a wide range of times, although deviations are evident at very long times. The variations seen at long times do not depend
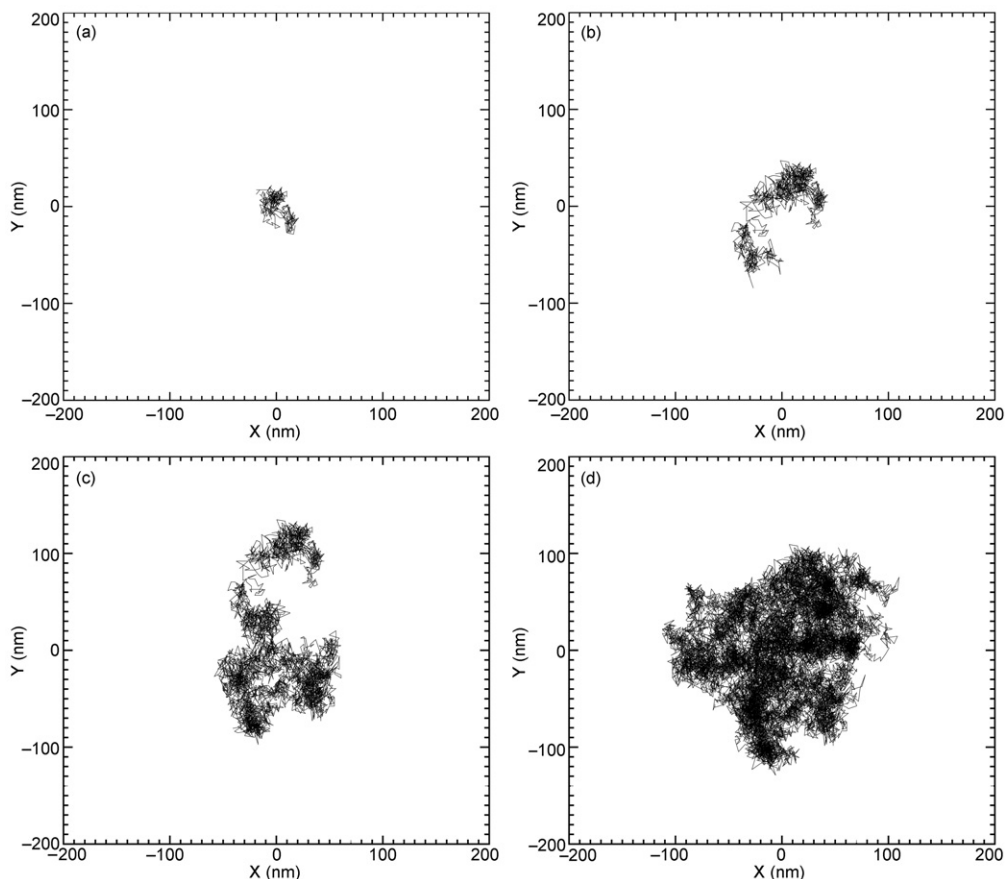
Fig. 3 The measured two-dimensional trajectory of one of two widely separated spheres in a semi-dilute PS solution ($c = 1.7\ c^*$) over a duration of (a) 0.0128 s, (b) 0.0512 s, (c) 0.2048 s, and (d) 0.8192 s. The sampling frequency is 20 kHz.

systematically on the pair spacing ρ and are probably a reflection of poor statistics or mechanical vibrations. The peak seen in $d_{ij}(t)$ is a consequence of the applied optical potential since for very long times the correlations between the two particles must decay ultimately back to zero.

The one- and two-particle mean-squared displacements contain features which originate from the viscoelasticity of the polymer solution and from the applied optical forces. To separate the two contributions we use the analysis of Section II. Inverting $d_{ii}(t)$ and $d_{ij}(t)$ yields friction coefficients which, apart from a simple scaling, do not depend on the applied potential. The computed friction coefficients are shown in the inset in Fig. 6. The frequency dependence seen is in sharp contrast to that expected for a purely viscous fluid where $\tilde{\xi}_{ij}$ remains independent of frequency. The steady decrease in the particle friction with increasing frequency reflects the viscoelasticity of the polymer solution and in particular its ability to store energy elastically at high frequencies. To discuss further the connection between the particle friction and the medium rheology we focus on the frequency scaled functions $s\tilde{\xi}_{ii}$ and $-s\rho\tilde{\xi}_{ij}$. In the continuum model of Levine and Lubensky[8,17] both functions are predicted to be simple multiples of the Laplace-transformed shear modulus $\tilde{G}(s)$ so that the ratio $-s\rho\tilde{\xi}_{ij}/s\tilde{\xi}_{ii}$ should be frequency-independent and from, eqns. (8) and (9), equal to 3/2. The experimentally-derived values for $s\tilde{\xi}_{ii}$ and $-s\rho\tilde{\xi}_{ij}$ are shown in Fig. 6. In partial accord with these predictions, we find that the two scaled friction coefficients do exhibit a very similar functional form (except possibly at the highest frequencies). However the ratio $-s\rho\tilde{\xi}_{ij}/s\tilde{\xi}_{ii}$ is not 3/2 but of order unity.
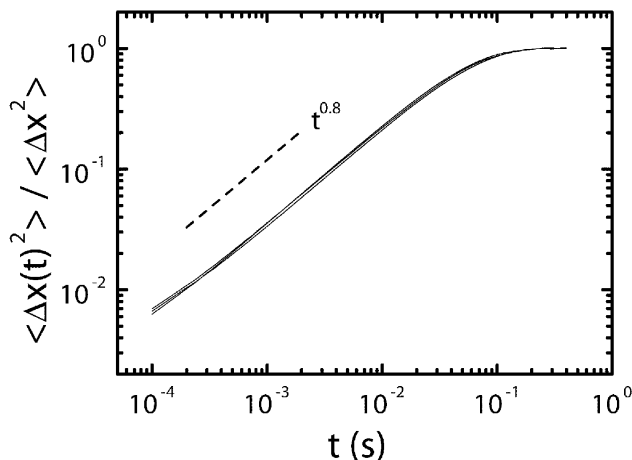
Fig. 4 Single particle mean squared displacements measured for a pair of widely-separated particles ($c = 1.7$ c^*). The different curves depict data collected at three different pair separations ranging from $\rho = 4.53$ to 16.96. No systematic variation with ρ is evident.
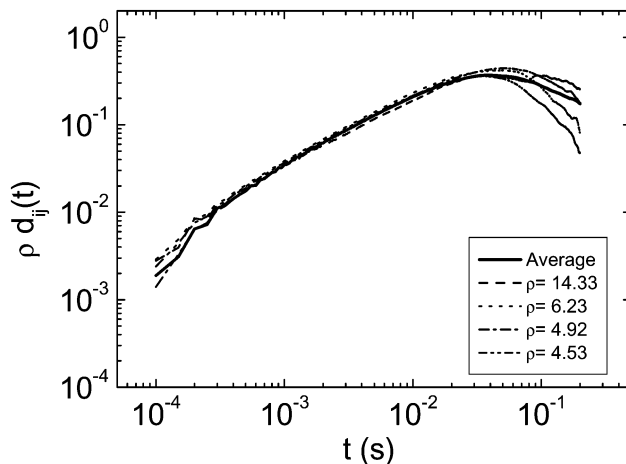
Fig. 5 The time dependence of the scaled mutual two-particle mean squared displacement $\rho d_{ij}(t)$ measured at four different pair separations ρ ($c = 1.7$ c^*). For intermediate times all of the data collapse onto a common curve showing that the strength of the two particle correlations varies inversely with the pair spacing ρ. The solid line is the average for all of the data collected.

    While we do not have a complete understanding of this discrepancy one possible explanation is that the nature of the shear coupling between the particle and the medium differs in the one- and two-particle situations. In the immediate vicinity of a probe particle a depletion zone exists with a reduced polymer segment concentration. While hydrodynamic forces will still couple the motion of the probe particle to the polymer matrix, the depletion zone could modify the nature of the boundary conditions at the particle surface. For a rigid spherical particle, the choice of boundary conditions changes the friction coefficient by a factor of $3/2$ from $6\pi\eta a$ for stick to $4\pi\eta a$ for slip.[9] Cardinaux et al.[18] have recently suggested that a slip, as opposed to a stick, boundary condition might apply to single particle motion in giant-micellar solutions. Assuming the depletion of polymer has a similar effect, then we should identify $\tilde{\xi}_{ii}(s)$ with $4\pi a\tilde{G}(s)/s$ rather than eqn. (8). In the
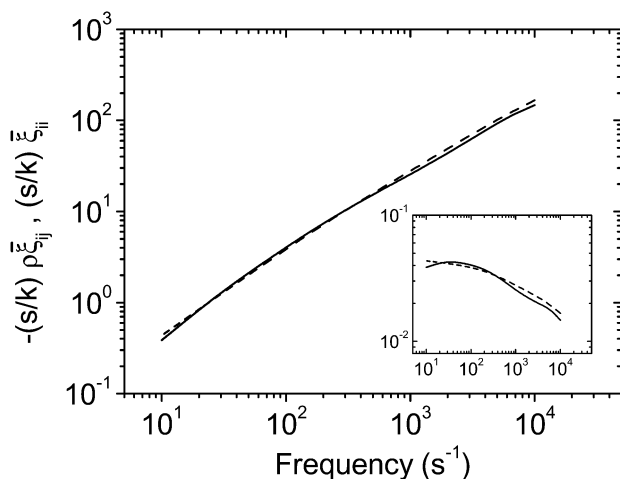
Fig. 6 Comparison of the frequency dependence of the scaled two-particle $-(s/k)\rho\tilde{\xi}_{ij}(s)$ (solid) and single-particle friction coefficients $(s/k)\tilde{\xi}_{ii}(s)$ (dashed) determined from the correlated fluctuations of two widely-spaced particles in a semi-dilute ($c = 1.7\ c^*$) polymer solution. The inset diagram shows $-(\rho/k)\tilde{\xi}_{ij}(s)$ (solid) and $\tilde{\xi}_{ii}(s)/k$ (dashed) as a function of frequency.

case of slip, the two-particle friction coefficient ξ_{ij} is given by[19] $-\rho\tilde{\xi}_{ij}(s) = 4\pi a\tilde{G}(s)/s$. In this case the ratio $-\rho\tilde{\xi}_{ij}/\tilde{\xi}_{ii}$ is 1.0 which is in close agreement with the value found experimentally. Further experimental and theoretical work is necessary to confirm this picture. A detailed comparison between the one- and two-particle friction coefficients as a function of polymer concentration and molecular weight is currently underway and will be the subject of future publications.

The frequency-dependent complex shear modulus $G^*(\omega) = G'(\omega) + iG''(\omega)$ may be determined from either the one- (after allowing for the slip boundary conditions) or two-point friction coefficients. Fig. 7 shows the storage and loss moduli computed from tweezer measurements for a 2.9 c^* solution of polystyrene. The data exhibit the features expected for an entangled flexible polymer solution.[10] At high frequencies, above the maximum relaxation time of the solution, the shear and loss moduli are expected to show a power law dependence on ω. Under Θ-conditions, G' and G''
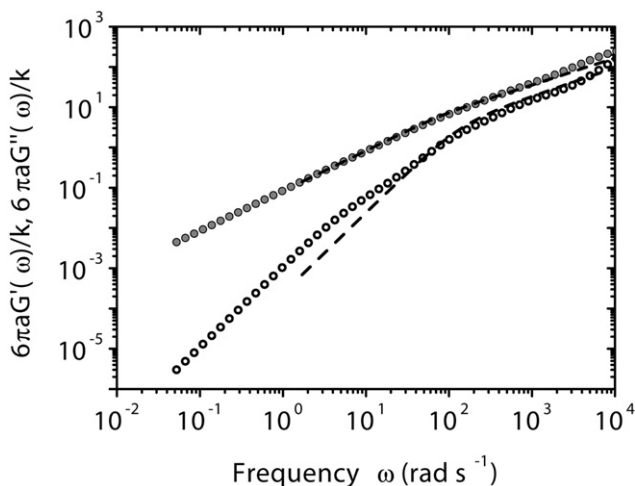
Fig. 7 Scaled storage $6\pi a G'(\omega)/k$ (open circles) and loss moduli $6\pi a G''(\omega)/k$ (filled circles) as function of frequency for 2.9 c^* solution of polystyrene in decalin. The dashed lines show predictions from Zimm theory.

are predicted by the Zimm model to vary as $\omega^{2/3}$. Fig. 7 shows that at high frequencies the complex modulus $G^*(\omega)$ follows closely the predictions of Zimm theory. At low frequencies the elasticity of the entanglement network contributes and the measured $G'(\omega)$ is increased above the Zimm predictions as expected for a semi-dilute solution.

V. Summary

In this paper we have demonstrated that combined measurements of one- and two-particle thermal fluctuations can be used to provide new insights into the the nature of the interface around a probe sphere embedded in a viscoelastic medium. We have measured the correlated Brownian motion of two widely-separated spheres held by a pair of tightly-focused laser beams within a polymer solution. Photodetection of scattered light was used to record the trajectories of the trapped particles with high spatial and temporal resolution. This new technique differs from previous two-point microrheological studies[7] in its spatial resolution and access to high frequencies; frequencies up to 10^4 rad s^{-1} are readily detectable. In comparison, the frequency range of previous two-point measurements[7] have been limited by the speed of video microscopy to $\omega \sim 10^2$ rad s^{-1}. Faster A/D data acquisition should enable the optical tweezer technique to be extended to still higher frequencies approaching 10^7 rad s^{-1}.

In order to achieve good statistics on two-particle correlations we have used a significantly higher-powered laser beam than previous (single-particle) optical tracking studies.[1,3,4] As a result we are no longer able to ignore the effects of optical forces applied by the laser beam on the measured particle fluctuations, as previous studies have assumed implicitly.[1,3,4] We account for the optical-gradient forces by analysing the dynamics of two harmonically-bound particles embedded in a general viscoelastic medium. By making two simplifying assumptions, which we show are valid in our experiments, we develop simple expressions for the frequency-dependent single- and two-particle friction coefficients, in terms of measurable quantities. We expect the single-particle friction coefficient to be sensitive to the rheological properties of the interfacial zone immediately surrounding a probe sphere while two-point measurements should allow the bulk rheological properties to be determined.

We have demonstrated the validity of our approach by analysing the one- and two-point correlations measured for 1.28 μm diameter poly(methyl methacrylate) spheres suspended in a semi-dilute solution of polystrene. One- and two-particle friction coefficients are computed. We confirm that over a wide range of particle separations, the two-point correlations vary inversely with the particle spacing r while the one-point correlations are independent of r. The two friction coefficients show a very similar dependence on frequency with the single-particle friction coefficient $\tilde{\xi}_{ii}(s)$ approximately equal to the corresponding two-particle friction coefficient $-\rho\tilde{\xi}_{ij}(s)$. While viscoelastic theory confirms that the two functions should have a similar frequency dependence, the ratio measured is in quantitative disagreement with recent theoretical calculations for a viscoelastic continuum,[8] which predict a ratio of $3/2$. We suggest that this discrepancy reflects the existence of a depletion zone around each particle in a non-adsorbing polymer solution. As a consequence, the shear coupling between particle and medium may be approximated by a slip rather than a stick boundary condition on the particle surface. With this assumption, either the one- or two-particle friction coefficients can be used to obtain the bulk rheology.

Acknowledgements

References

1 S. Yamada, D. Wirtz and S. Kuo, *Biophys. J.*, 2000, **78**, 1736.
2 T. G. Mason and D. A. Weitz, *Phys. Rev. Lett.*, 1995, **74**, 1250.
3 T. G. Mason, K. Ganesan, J. H. van Zanten, D. Wirtz and S. C. Kuo, *Phys. Rev. Lett.*, 1997, **79**, 3282.

4   (a) F. Gittes, B. Schnurr, P. D. Olmsted, F. C. MacKintosh and C. F. Schmidt, *Phys. Rev. Lett.*, 1997, **79**, 3286; (b) B. Schnurr, F. Gittes, F.C. MacKintosh and C. F. Schmidt, *Macromolecules*, 1997, **30**, 7781.
5   M. J. Solomon and Q. Lu, *Curr. Opin. Colloid Interface Sci.*, 2001, **6**, 430.
6   F. G. Schmidt, B. Hinner and E. Sackmann, *Phys. Rev. E*, 2000, **61**, 5646.
7   J. C. Crocker, M. T. Valentine, E. R. Weeks, T. Gisler, P. D. Kaplan, A. G. Yodh and D. A. Weitz, *Phys. Rev. Lett.*, 2000, **85**, 888.
8   (a) A. J. Levine and T. C. Lubensky, *Phys. Rev. E*, 2001, **65**, 011 501; (b) A. J. Levine and T. C. Lubensky, *Phys. Rev. Lett.*, 2000, **85**, 1774.
9   J. P. Hansen and I. R. McDonald, *Theory of Simple Liquids*, Academic Press, London, 2nd edn., 1986.
10 M. Doi and S. F. Edwards, *The Theory of Polymer Dynamics*, Oxford University Press, Oxford, 1988.
11 (a) S. Henderson, S. Mitchell and P. Bartlett, *Phys. Rev. Lett.*, 2002, **88**, 088 302; (b) S. Henderson, S. Mitchell and P. Bartlett, *Phys. Rev. E*, 2001, **64**, 061 403; (c) S. Henderson, S. Mitchell and P. Bartlett, *Colloids Surf. A*, 2001, **190**, 81.
12 J. B. Avalos, J. M. Rubi and D. Bedeaux, *Macromolecules*, 1991, **24**, 5997.
13 G. K. Batchelor, *J. Fluid. Mech.*, 1976, **74**, 1.
14 W. Press, S. A. Teukolsky, W. T. Vetterling and B. P. Flannery, *Numerical Recipes in FORTRAN*, Cambridge University Press, Cambridge, 2nd edn., 1992.
15 S. W. Provencher, *Comput. Phys. Commun.*, 1982, **27**, 213.
16 G. C. Berry, *J. Chem. Phys.*, 1966, **44**, 4550.
17 A. J. Levine and T. C. Lubensky, *Phys. Rev. E*, 2001, **63**, 041 510.
18 F. Cardinaux, L. Cipelletti, F. Scheffold and P. Schurtenberger, *Europhys. Lett.*, 2002, **57**, 738.
19 R. B. Jones, personal communication, 2002.